JOURNAL OF VIROLOGY, Apr. 1997, p. 3208–3218 Vol. 71, No. 4
0022-538X/97/$04.00+0

Characterization of Borna Disease Virus p56 Protein, a Surface Glycoprotein Involved in Virus Entry†

DANIEL GONZALEZ-DUNIA,[1] BEATRICE CUBITT,[1] FRIEDRICH A. GRÄSSER,[2] AND JUAN CARLOS DE LA TORRE[1]*

Division of Virology, Department of Neuropharmacology, The Scripps Research Institute, La Jolla, California 92037,[1] and Abteilung Virologie, Institut für medizinische Mikrobiologie und Hygiene, Universitätskliniken des Saarlandes, 66421 Homburg, Germany[2]

Received 28 October 1996/Accepted 17 December 1996

Borna disease virus (BDV) is a nonsegmented negative-stranded (NNS) RNA virus, prototype of a new taxon in the *Mononegavirales* order. BDV causes neurologic disease manifested by behavioral abnormalities in several animal species, and evidence suggests that it may be a human pathogen. To improve our knowledge about the biology of this novel virus, we have identified and characterized the product of BDV open reading frame IV (BVp56). Based on sequence features, BVp56 encodes a virus surface glycoprotein. Glycoproteins play essential roles in the biology of NNS RNA viruses. Expression of BVp56 resulted in the generation of two polypeptides with molecular masses of about 84 and 43 kDa (GP-84 and GP-43). GP-84 and GP-43 likely correspond to the full-length BVp56 gene and to its C terminus, respectively. Endoglycosidase studies demonstrated that both products were glycosylated and that this process was required for the stabilization of newly synthesized products. Moreover, our results suggested that GP-43 is generated by cleavage of GP-84 by a cellular protease. Subcellular localization studies demonstrated that GP-84 accumulates in the ER, whereas GP-43 reaches the cell surface. Both BVp56 products were found to be associated with infectious virions, and antibodies to BVp56 had neutralizing activity. Our findings suggest that BVp56 exhibits a novel form of processing for an animal NNS RNA virus surface glycoprotein, which might influence the assembly and budding of BDV.

Borna disease virus (BDV) causes central nervous system (CNS) disease in several vertebrate species, manifested by behavioral abnormalities and diverse pathology (18, 26, 32). BDV is a nonsegmented negative-stranded (NNS) RNA virus, with a genomic organization similar to that of other members of the *Mononegavirales* order (4, 10). However, in contrast to the other known animal NNS RNA viruses, BDV replication and transcription occur in the nucleus (3, 9). Moreover, BDV uses RNA splicing for the regulation of its gene expression (11, 39). These findings have led to the proposal that BDV represents the prototype of a new family of animal NNS RNA viruses (12, 38).

Sensitivity to detergents and organic solvents suggested that BDV is an enveloped virus (27). This has been further supported by electron microscopy data, showing the presence of enveloped particles with a size of approximately 100 nm in the cytoplasm of BDV-infected cells (8), as well as in cesium chloride gradient preparations of cell-free BDV infectious particles (54).

Viral glycoproteins (GP) present at the surface of enveloped viruses have important functions (reviewed in reference 37). They mediate virus attachment to the cell surface receptors and facilitate penetration by triggering fusion of the viral envelope with cell membranes. Therefore, these GPs are primary determinants of viral tropism. Also, viral GPs participate in the assembly and budding of new virions and are often essential in determining the site for virus maturation, since their retention in a given intracellular compartment can play a decisive role in the localization of the virus maturation site (31). In addition, viral GPs are often the main target for the immune response of an infected host (37).

Virus surface GPs have been extensively studied for other known NNS RNA viruses, comprising the families *Paramyxoviridae*, *Filoviridae*, and *Rhabdoviridae* (14). *Paramyxoviridae* possess two integral membrane proteins, one of which (HN) is involved in cell attachment and the other of which (F) is involved in mediating pH-independent fusion of the viral envelope with cellular membranes (25). Filoviridae have a single GP making up the virion surface spike (30). Expression of this GP results from a complex regulatory mechanism involving both transcriptional editing and translational frameshifting (35). Finally, *Rhabdoviridae* also have a single GP present at the surface of the virus (44). In all cases, synthesis of these GPs involves maturation by trafficking through the Golgi complex. Eventually, these GPs are expressed at the cell surface and assembly of infectious virions occurs through budding on plasma membranes.

Among the five major open reading frames (ORF) predicted in the BDV genome sequence (4, 10, 12, 38), sequence features indicate that ORF IV (BVp56) is likely the counterpart of the virus surface glycoprotein found in other NNS RNA viruses. However, no information is presently available about the expression of BVp56 and its role in the virus life cycle. Little or no infectious virus is released from BDV-infected cells (18, 26, 32) and recognition of BDV GP by sera of infected animals has not been reported yet. Moreover, electron microscopy data suggest that BDV does not appear to maturate at the plasma membrane (8). All of these features are unusual for a NNS RNA virus, stressing the importance of elucidating the expres-

* Corresponding author. Mailing address: Division of Virology, Department of Neuropharmacology, The Scripps Research Institute, 10550 N. Torrey Pines Rd., La Jolla, CA 92037. Phone: (619) 784-9462. Fax: (619) 784-9981. E-mail: juanct@scripps.edu.

† Publication 10395-NP from The Scripps Research Institute.

sion and function of BVp56 to understand the biology of BDV better.

Here, we show that expression of BVp56 in BDV-infected cells results in two glycosylated products (GP-84 and GP-43). GP-84 likely corresponds to the full-length product encoded by ORF IV, and GP-43 is derived from the C terminus of GP-84, presumably by cleavage by a cellular protease. Studies of the sensitivity to endoglycosidases show that both GP-84 and GP-43 retain endoglycosidase H sensitivity. Moreover, GP-84 accumulates in the endoplasmic reticulum (ER) whereas GP-43 reaches the cell surface. We also show that both products are associated with infectious virions and are involved in the initiation of infection by BDV. These features are indicative of a novel mechanism for the processing of a NNS RNA virus surface GP and hence for the assembly of BDV particles.

MATERIALS AND METHODS

Construction of expression vectors and recombinant vaccinia viruses. All vectors for the expression of BDV p56 were obtained from a BDV cDNA clone, spanning nucleotides 1760 to 4690 of the BDV genome (10). Analysis of the BVp56 gene sequence was performed by using the Genetics Computer Group (Madison, Wis.) software package. A DNA fragment corresponding to full-length ORF IV (BVp56) was produced by PCR with primers BV2225F (5′-CG AATTCGCACGCAATTAATGCAGC-3′) and BV3738R (5′-GCTACTCGAG CGGTACGGTTTATTCCTGC-3′). The numbers of the primers used in this study refer to the hybridization positions in the BDV genomic sequence (10) and F and R stand for forward and reverse primer, respectively, with respect to the BDV antigenomic (sense) polarity. The resulting fragment was cloned in pCRII plasmid (InVitrogen, La Jolla, Calif.).

A recombinant BVp56 gene, tagged on its C terminus with a 10-amino-acid epitope (EQKLISEEDL) from the c-*myc* proto-oncogene (BVp56-*myc*), was constructed in a single step patch-PCR as described previously (41). This approach relies on the simultaneous use of three primers, including a patch primer that bridges the p56 and *myc* coding regions. We used primer BV2225F, together with the 45-mer 3′ patch primer 5′-CTCAGAAATCAGCTTTTGCTCACCTC CTTCCTGCCACCGGCCGAG-3′. This primer codes for the complementary sequence to the five C-terminal amino acids of BVp56, followed by amino acids of human c-*myc*, and includes a Gly-Gly bridge between these sequences. Finally, the third 42-mer 3′ primer, 5′-GCACTCGAGTTACTACAGATCCTCCTCAG AAATCAGCTTTTG-3′, consists of 18 nucleotides identical to the patch primer and a tail sequence encoding the last three amino acids of the c-*myc* epitope, a termination codon, and a unique *Xho*I restriction site. Conditions for PCR were as described previously (41), and the product was cloned into pCRII and verified by sequencing.

To construct recombinant vaccinia viruses, the BVp56 and BVp56-*myc* genes were subcloned into the pVVT1 transfer vector. pVVT1 is a modified version (49a) of the previously described pSC11 vector (6). Procedures for gene introduction and selection of recombinant vaccinia viruses were essentially as described (50, 51). The recombinant vaccinia virus expressing T7 RNA polymerase (vTF7-3, designated VVT7 in this study) was kindly provided by B. Moss.

The BVp56Δ expression vector was constructed by PCR by using primers BV2225F and primer BV2857R (5′-CTATCAACGCCTGAATTCATCGAAG GAAAC-3′) and cloning of the amplified fragment into pCRII. BVp56Δ contains the first 217 amino acids of BVp56 cloned downstream of the T7 RNA polymerase promoter. This allows for expression by using the VVT7 infection/transfection system as described previously (1, 15). In addition, the full-length BVp56 gene was also subcloned in the pRC/CMV vector (InVitrogen) immediately downstream of the cytomegalovirus (CMV) promoter. The resulting vector was designated CMV-p56.

Generation of rabbit antiserum to BVp56. To raise a BVp56-specific rabbit antiserum, we expressed a truncated form of BVp56 (trpE-BVp56) as a TrpE fusion protein in *Escherichia coli* by using the pATH2 vector system (24). We used a truncated BVp56 protein after experiencing difficulties in expressing the full-length BVp56 in *E. coli*. Primers 5′-CCCCCCGGGCAATGTACTGCAGT TTCGCGGACT-3′ and 5′-GGGCCCGGGTTATTCCTGCCACCGGCCGA -3′ were used to generate by PCR an N-terminal-truncated form of the p56 protein starting at a methionine residue located in position 150. Protein extracts from bacteria expressing the trpE-BVp56 fusion protein were separated by sodium dodecyl sulfate-polyacrylamide gel electrophoresis (SDS-PAGE). The recombinant protein was eluted from the gel and emulsified in complete or incomplete Freund's adjuvant. Procedures for immunization of rabbits and collection of antisera were as described previously (36).

Cell lines and viruses. The rat glioma cell line C6 (ATCC CCL 107) and human neuroblastoma SKNMC cells (ATCC HTB 10) were persistently infected with BDV as described previously (5) and designated C6BV and SKNMC/BV, respectively. BHK-21 (ATCC CCL 10), C6 and C6BV cells were maintained in high-glucose Dulbecco's modified eagle medium (DMEM) supplemented with 2 mM glutamine and 10% heat-inactivated fetal calf serum (FCS). SKNMC and SKNMC/BV cells were grown in Iscove's medium (Sigma, St. Louis, Mo.) with 1× Bufferall, 1× nonessential amino acids, 2 mM sodium pyruvate, 2 mM glutamine, and 15% FCS. Vaccinia viruses were amplified on HeLa cells grown in DMEM containing 7% FCS and 2 mM glutamine. Titration of vaccinia viruses was done by plaque assay on BHK-21 cells.

For vaccinia infection, 80% confluent BHK-21 cell monolayers in 35-mm dishes were infected with the recombinant vaccinia viruses at a multiplicity of infection of 5 PFU/cell. After a 1-h adsorption period, the inoculum was replaced by culture medium. Transfections were carried out by using Lipofectamine (GibcoBRL, Grand Island, N.Y.) and Quiagen-prepared plasmid DNA (Quiagen, Chatswoth, Calif.) as described previously (17). For vaccinia virus T7-driven expression, cells were infected with VVT7 virus and transfected with the plasmid DNA after the adsorption period. Whole-cell extracts were prepared 16 h after transfection.

RNA extraction and Northern blot analysis. Total RNA was isolated from cultured cells with TRI-Reagent (Molecular Research Center, Cincinnati, Ohio). Poly(A)$^+$ RNA was purified by two rounds of oligo(dT) cellulose chromatography (9). RNA samples were analyzed by Northern blot hybridization, using procedures described elsewhere (17).

Western blot analysis. Cell lysates were separated by SDS-PAGE (10% polyacrylamide) by using the buffer system of Laemmli, and the proteins were transferred onto Immobilon-P membranes (Millipore, Bedford, Mass.) as described previously (34). Immunodetection of proteins was done by using the BM Chemiluminescence kit (Boehringer Mannheim, Indianapolis, Ind.), as recommended by the manufacturer.

Subcellular fractionation. Adherent cells were washed twice with phosphate-buffered saline (PBS) and dissociated with nonenzymatic dissociation solution (Sigma). Nuclei and cytoplasm were partitioned after disruption of the plasma membrane with 0.5% Nonidet P-40 as described previously (9). For the preparation of microsomal membranes, cells were suspended in DHB buffer (10 mM HEPES, 1 mM $MgCl_2$, supplemented with protease inhibitors) and disrupted with a Dounce homogenizer (15 strokes). Cell homogenates were layered on a 10% sucrose cushion in DHB. After centrifugation (18,000 × *g* for 4 h at 4°C), the microsomal pellet was dissolved in 50 mM triethanolamine, pH 7.5. Equivalent amounts of each subcellular fraction were analyzed by Western blot.

Treatment with enzymes and chemicals. Tunicamycin (TUN) (1 μg/ml) (Calbiochem, La Jolla, Calif.) cycloheximide (30 μg/ml) (Sigma), or brefeldin A (10 μg/ml) (Epicenter Technologies, Madison, Wis.) was added to the tissue culture supernatant. Cell extracts were prepared at different times after onset of treatment. TUN and brefeldin A were added to BHK-21 cells 1 h before infection with the vaccinia recombinants and maintained throughout infection. Protease inhibitors (2 mM phenylmethylsulfonyl fluoride, 2 μg of aprotinin per ml, and 1 μg of leupeptin per ml, all from Sigma) were also added to the medium of treated cells.

Endoglycosidase F and H digestions were performed essentially as described previously (29). An aliquot of the microsome preparation from SKNMC or SKNMC/BV cells was precipitated with 2 volumes of methanol and 2 volumes of acetone (1), pelleted by centrifugation at 10,000 × *g* for 30 min, and resuspended in the glycosidase digestion buffers. Reactions were carried out with or without 0.2 U of endoglycosidase F (Endo F) or 2 mU of Endo H (both from Boehringer Mannheim), for 18 h at 37°C. Samples were then separated by SDS-PAGE and analyzed by Western blot.

Immunofluorescence. Cells grown on coverslips were fixed with methanol-acetone and processed for immunofluorescence as described previously (9). Briefly, after blocking with 10% normal goat serum for 45 min at room temperature, cells were stained with primary antibodies, i.e., the rabbit antisera anti-BVp56 or anti-BVp40 (36). We also used the SPA-827 mouse monoclonal antibody (Stressgen, Victoria, British Columbia, Canada), specific for Grp78 (BiP), an ER resident protein, as well as a rabbit anti-mannosidase II antibody, a Golgi complex marker (a gift from M. G. Farquhar). Secondary fluorescent antibodies used were fluorescein isothiocyanate (FITC)-labeled anti-rabbit immunoglobulin G (IgG) and Texas Red-labeled anti-mouse IgG (Cappel, West Chester, Pa.). For colocalization studies, cells were examined with a BioRad MRC600 confocal microscope.

Biotinylation of cell surface proteins. Cells grown on six-well plates were washed four times in cold PBS supplemented with 0.1 mM $CaCl_2$ and 1 mM $MgCl_2$ (PBS-CM). Surface-specific biotinylation was accomplished by addition of 1 ml of 0.5 mg/ml NHS-SS-biotin diluted in PBS-CM (Pierce, Rockford, Ill.) as described previously (40). Briefly, the reagent was reacted twice for 30 min at 4°C with gentle shaking. Free biotin was quenched by washing twice with DMEM and twice with PBS-CM. The cells were lysed in 1 ml of lysis buffer (150 mM NaCl, 1% Nonidet P-40, 1% sodium deoxycholate, 0.1% SDS, 50 mM Tris, pH 8.0), and lysates were clarified by centrifugation (10,000 × *g*, 10 min at 4°C). To separate the biotinylated surface proteins, the cell lysates were incubated with 60 μl of a 50% suspension of streptavidin-agarose for 16 h at 4°C. After binding, the agarose beads were washed four times in lysis buffer and bound proteins were eluted by boiling in SDS-PAGE sample buffer. In each case, an identical sample was reacted in parallel with NHS-SS biotin and directly eluted in sample buffer to provide a whole-cell extract control. Samples were then analyzed by Western blot. To provide a control for the detection of a protein expressed at the surface,

we used a monoclonal antibody specific for the transferrin receptor (antibody H-68; a gift from I. Trowbridge).

Preparation of cell-free virus and infectivity assays. SKNMC/BV cell monolayers were subjected to a 60-min hypertonic treatment (20 mM Tris, pH 7.4, 250 mM $MgCl_2$) at 37°C to promote the release of cell-bound virus. The supernatant was clarified (2,500 × *g* for 5 min at 4°C) twice, adjusted to 0.002% Zwittergent 3-14 (Calbiochem), and incubated for 30 min at 20°C, and virus particles were pelleted through a 15% sucrose cushion at 100,000 × *g* for 1 h at 4°C. The virus pellet was resuspended in PBS with 2% FCS and layered onto a step Renografin gradient (consisting of 2 ml of 75% Renografin and 1.5 ml of each 40% and 20% Renografin). Renografin solutions were made in 10 mM HEPES, pH 7.4, and 75 mM NaCl. Samples were centrifuged at 36,000 rpm for 2 h at 4°C in a Beckman SW40 Ti rotor. The banded material present at the interface between 40% and 20% Renografin was collected, diluted with three volumes of 10 mM HEPES, pH 7.4–75 mM NaCl, and layered onto a preformed 25 to 45% continuous Renografin gradient prepared in the same solution. Samples were centrifuged at 40,000 rpm for 6 h at 4°C in a Beckman SW40 Ti rotor. The gradient fractions were collected, and their densities were determined by weighing. The infectivity of each fraction was determined by an immunofocus assay on C6 cells grown on coverslips as described previously (9). Focus-forming units (FFU) were counted by examination of the samples with a fluorescence microscope. For neutralization experiments, virus fractions were incubated with serial dilutions of heat-inactivated antisera for 1 h at 37°C before the immunofocus assay was performed. Aliquots of the virus-containing fractions were also spotted onto carbon-coated grids, stained with uranyl acetate (20), and examined by electron microscopy.

RESULTS

BVp56 predicted structure and gene expression. The predicted amino acid sequence (12, 38) of BVp56 consists of 503 amino acids with a molecular mass of 56,505 Da. It shows a relatively high content of asparagine, serine, and threonine residues (20.7%), resulting in the presence of 13 Asn-X-Thr/Ser motifs (Asn positions 63, 109, 139, 192, 196, 202, 221, 230, 235, 321, 328, 388, and 438) that are putative sites for N glycosylation. Several potential phosphorylation sites are also predicted in the BVp56 sequence. BVp56 contains two strong hydrophobic domains, one located at the N-terminal and the other at the C-terminal end of the polypeptide. These domains are reminiscent of the signal sequence and transmembrane domain, respectively, found in other NNS RNA viruses GPs (37). These features indicate that BVp56 likely belongs to the type I of integral membrane proteins (52), with its N terminus protruding towards the outside and a short C-terminal cytoplasmic domain. Comparisons using the BestFit program failed to identify any similarity of BVp56 with GPs of any other NNS RNA virus.

BDV utilizes RNA splicing to generate some of its messenger RNAs (11, 39). While the BDV nucleoprotein (BVp40) and phosphoprotein (BVp24) gene products are translated from monocistronic unspliced mRNAs (see Fig. 1A), the other viral polypeptides, including BVp56, are predicted to be translated from polycistronic unspliced or spliced mRNAs (11, 39). To identify which mRNA species could encode BVp56 in SKNMC/BV cells, poly(A)$^+$ RNA was isolated from BDV-infected and uninfected control cells and analyzed by Northern blot hybridization using a BVp56-specific probe (Fig. 1). Consistent with previous reports (11, 39), we did not detect a monocistronic RNA encoding BVp56 (Fig. 1B, lane 4). Moreover, results from Northern blot hybridization using a BVp16 probe indicated that all the mRNA species that can potentially encode BVp56 start upstream of the BVp16 gene, at the transcription initiation site S3 (Fig. 1A; Fig. 1B, lane 2).

Expression of BVp56 in BDV-infected cells. Two polypeptides with apparent molecular masses of 84 and 43 kDa (GP-84 and GP-43) were detected in BDV-infected cells by Western blot, using a rabbit antiserum (RbαBVp56) raised against a recombinant trpE-BVp56 fusion protein expressed in *E. coli* (Fig. 2). GP-84 and GP-43 were detected in SKNMC/BV and in C6BV cells but not in their parental noninfected cell lines (compare lanes 1 and 2 in Fig. 2A and B). These polypeptides were not detected with the preimmune rabbit serum (not shown). The same two polypeptides were detected in BHK-21 cells infected with a recombinant vaccinia virus expressing BVp56 (VV-BVp56) but not with VVT7 virus expressing the T7 RNA polymerase (Fig. 2A, lanes 3 and 4). This indicates that all the information required for the production of both GP-84 and GP-43 polypeptides is contained in the BVp56 gene, encoded by ORF IV in the BDV genome. Additional bands were detected in BDV-infected as well as in uninfected cells and in cells infected with VVT7 virus and were considered evidence of nonspecific binding of the RbαBVp56 antiserum.

We also infected BHK-21 cells with a recombinant vaccinia virus expressing BVp56 tagged on its C terminus with a c-*myc* epitope (VV-BVp56-myc). In this case, we observed a shift in the mobility of both GP-84 and GP-43 polypeptides (Fig. 2A, lane 5). In the case of GP-84 the effect of the addition of the c-*myc* epitope on electrophoretic mobility was better appreciated after a 10 to 20% gradient SDS-PAGE (data not shown). Since this epitope had been placed at the 3′ end of the BVp56 gene (Fig. 2E), it suggests that GP-43 corresponds to the C terminus of the full-length protein, represented by GP-84. Hence, GP-43 could be generated either by internal initiation in the BVp56 gene or by cleavage of GP-84. Internal initiation seems rather unlikely since there is no internal ATG codon in the BVp56 sequence consistent with the generation of GP-43, even after taking into account the possibility of glycosylation. In the case of a cleavage of GP-84 to generate GP-43, we should also expect a polypeptide corresponding to the N terminus of GP-84, with an estimated molecular mass of approximately 41 kDa. However, such a product was not detected in our samples.

Since the trpE-BVp56 protein used to generate the RbαBVp56 serum has a deletion of the first 150 amino acids of BVp56 (Fig. 2E), we wanted to rule out the possibility that our antiserum was unable to detect the predicted polypeptide of 41 kDa, corresponding to the N terminus of GP-84. For this purpose, we generated the BVp56Δ expression plasmid, containing amino acids 1 to 217 of BVp56 under the control of the T7 promoter. This construct has only 67 amino acids in common with trpE-BVp56 (Fig. 2E) and directs the synthesis of a polypeptide with a calculated molecular mass of 24 kDa. BHK-21 cells were infected with VVT7 and transfected with BVp56Δ, and whole-cell extracts were analyzed by Western blot. A polypeptide with a molecular mass of about 35 kDa was detected with the RbαBVp56 serum (Fig. 2C, lane 3). The molecular mass of this polypeptide, higher than predicted, is likely due to glycosylation, since BVp56Δ retains six potential glycosylation sites of the BVp56 sequence. Therefore, the lack of detection of the N-terminal fragment of GP-84 following cleavage is probably due to its rapid degradation.

Next, we studied the subcellular distribution of BVp56 products. SKNMC/BV cells were fractionated into nuclear, cytoplasmic, and microsomal fractions and analyzed by Western blot (Fig. 2D). Both GP-84 and GP-43 were present in the cytoplasm but not detected in the nuclear fraction. The two polypeptides were also detected in the microsome-enriched fraction, indicating an association of these proteins with membranes (cell surface and/or ER).

BVp56 is glycosylated. BVp56 has a length of 503 amino acids, with a predicted molecular mass of 56,505 Da. According to sequence features, the large apparent molecular mass of 84 kDa could be due to glycosylation of the BVp56 protein. To test this hypothesis, we treated BHK-21 cells with TUN, an inhibitor of N-linked glycosylation, before infection with recombinant vaccinia viruses expressing BVp56 and BVp40 gene

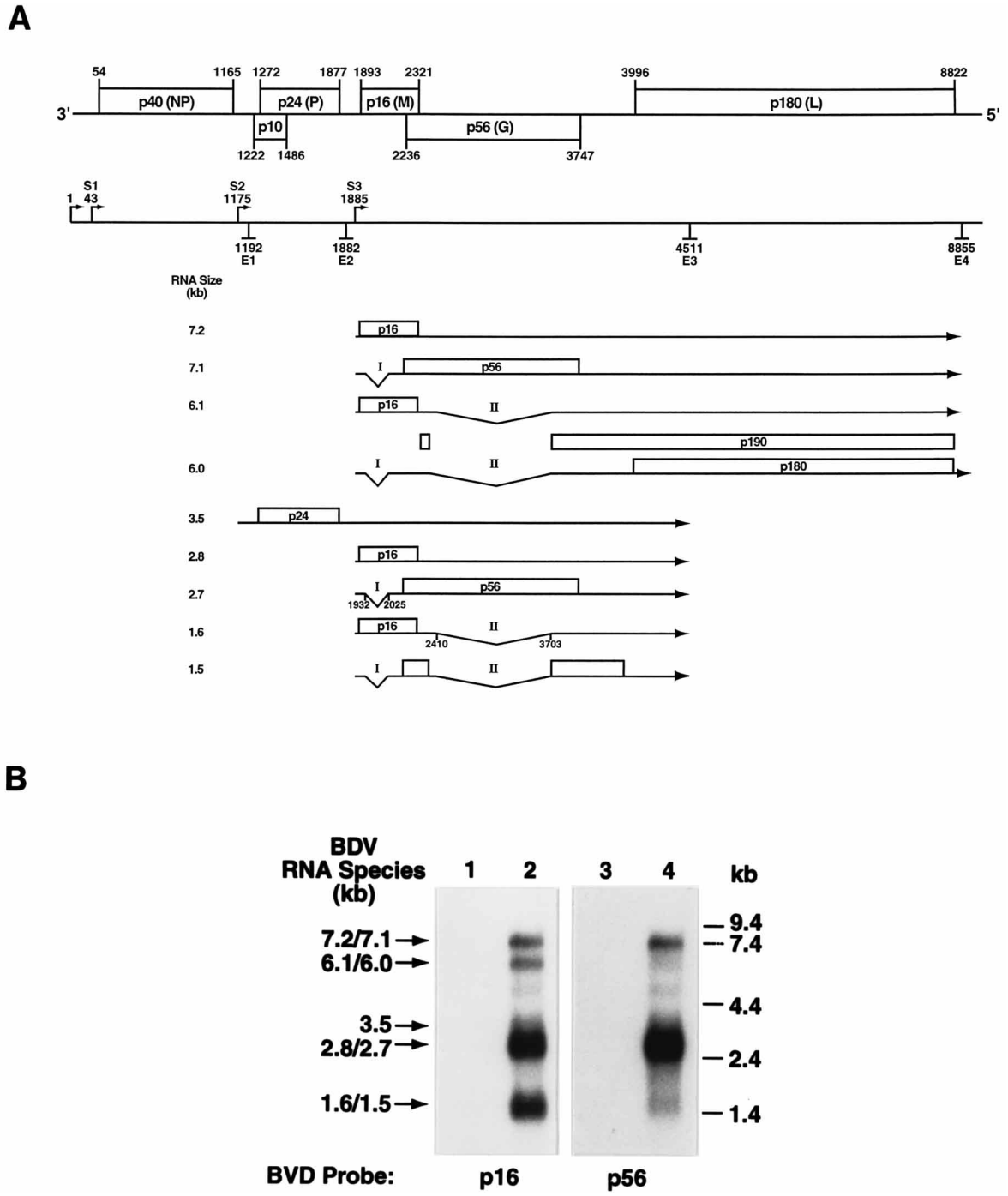

FIG. 1. BVp56 mRNA expression. (A) BDV transcription map. The upper part of the figure is a schematic representation of the genomic organization of BDV, as well as the positions of the start (S) and end (E) transcriptive signals. NP, P, M, G, and L refer to the positions of BDV putative nucleoprotein, phosphoprotein, matrix, GP, and polymerase genes, respectively. The two introns described in the BDV genome (11, 39) are designated I and II. All of the mRNAs that span the region of the genome containing BVp56 are indicated on the map, with their predicted sizes shown on the left. (B) Northern blot analysis. Poly(A)$^+$ RNA was isolated from SKNMC (lanes 1 and 3) and SKNMC/BV (lanes 2 and 4) cells. Hybridization was first performed with a BVp56-specific cDNA (lanes 3 and 4). The same blot was then stripped by boiling twice in 2 mM EDTA–5 mM Tris, pH 7.5–0.1% SDS and hybridized with a BVp16-specific cDNA (lanes 1 and 2). Two additional mRNA species (corresponding to the 6.1- to 6.0-kb and 1.6- to 1.5-kb mRNAs) were detected with this probe. Exposure time was 16 h at −80°C in each case. The position of RNA standards (RNA ladder; Gibco BRL, Grand Island, N.Y.) is shown on the right. Arrows indicate the expected sizes of the different BDV mRNAs.

products (Fig. 3A). Cells were harvested 18 h after infection in the presence of TUN and analyzed by Western blotting (Fig. 3A). We used this approach rather than metabolic labeling of BDV-infected cells in the presence of TUN followed by immunoprecipitation, because the RbαBVp56 antiserum did not work in immunoprecipitation assays. Expression of the BDV p40 protein, which is not glycosylated, was unaffected by such a treatment (compare lanes 5 and 6 in Fig. 3A). In contrast,

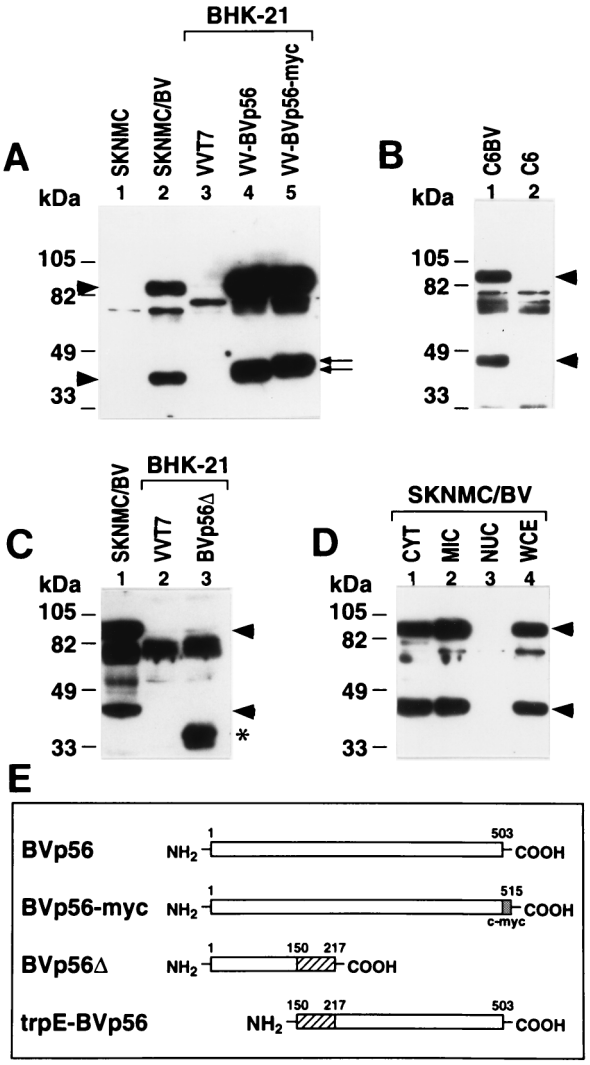

FIG. 2. Expression of BVp56 in BDV-infected cells. (A) Whole-cell extracts from SKNMC and SKNMC/BV cells, as well as from BHK-21 cells infected with VVT7, VV-BVp56 and VV-BVp56-myc recombinant vaccinia viruses (lanes 1 through 5, respectively), were prepared as described in Materials and Methods, separated by SDS-PAGE, transferred to an Immobilon-P membrane, and probed with the rabbit anti-BVp56 (RbαBVp56) antiserum, diluted 1:1,000. Detection of bound antibody, using a peroxidase-conjugated anti-rabbit antibody and a chemiluminescent substrate for the peroxidase, was performed as described in Materials and Methods. Arrowheads on the left indicate the positions of GP-84 and GP-43 polypeptides. Arrows on the right indicate the observed shifts in the mobility of GP-43 between lanes 4 and 5. (B) Western blot assay on whole-cell extracts from C6BV (lane 1) and C6 (lane 2) cells, using the RbαBVp56 antiserum. (C) Western blot assay using the RbαBVp56 antiserum performed on SKNMC/BV cell extracts (lane 1), as well as on extracts of BHK-21 cells infected with VVT7 virus (lanes 2 and 3) and transfected with the BVp56Δ construct (lane 3). The position of the polypeptide encoded by this construct is indicated with a star. (D) Subcellular fractionation. SKNMC/BV whole-cell extracts (WCE, lane 4) were partitioned into cytoplasmic (CYT), microsomal (MIC), and nuclear (NUC) fractions (lanes 1, 2, and 3, respectively). Equivalent amounts were analyzed by Western blotting using the RbαBVp56 antiserum. Arrowheads in panels B, C, and D indicate the positions of GP-84 and GP-43 polypeptides. (E) Schematic representation of the different constructs of the BVp56 gene used in this study.

expression of both GP-84 and GP-43 were not detected in the presence of TUN (compare lanes 3 and 4 in Fig. 3A).

To investigate the stability of GP-84 and GP-43 in BDV-infected cells, SKNMC and SKNMC/BV cells were treated with cycloheximide (CHX). After treatment with CHX for 24 h, levels of GP-84 started to decrease in SKNMC/BV cells, whereas GP-43 levels remained unaffected after treatment for up to 36 h (Fig. 3B).

We also studied the processing of GP oligosaccharide side chains by treatment with endoglycosidases. Aliquots of microsomal preparations from SKNMC and SKNMC/BV cells were digested with endoglycosidases and analyzed by Western blotting (Fig. 4A). Both GP-84 and GP-43 were sensitive to deglycosylation by using Endo F, which removes all forms of N-linked sugars. Endo F treatment generated polypeptides with molecular masses of about 56 and 27 to 29 kDa (compare lanes 3 and 4 in Fig. 4A). A similar pattern was observed after digestion with Endo H (compare lanes 5 and 6 in Fig. 4A). This enzyme removes carbohydrates only in the high-mannose form, before their maturation in the medial Golgi complex. These results indicate that the GP-84 and GP-43 proteins contain N-linked sugars which retain Endo H sensitivity.

To analyze the role of post-ER compartmentalization in the generation of BVp56 polypeptides, BHK-21 cells were treated with brefeldin A (BFA) before infection with recombinant vaccinia viruses (Fig. 4B). BFA is a macrocyclic lactone that causes recycling of Golgi cisternae to the ER and completely blocks membrane traffic out of the ER (43). As shown in Fig. 4B, the mobility of GP-84 was slightly affected by BFA treatment (compare lanes 1 and 2). This is probably due to a blockade in the late stages in the glycosylation process that has already been described for other viral GP in BFA-treated cells (7). Interestingly, the generation of GP-43 was completely blocked in BFA-treated cells, suggesting that GP-43 production is posterior to that of GP-84 and requires trafficking in a post-ER compartment. In contrast, we observed that production of the BVp40 protein was unaffected by BFA (compare lanes 5 and 6 in Fig. 4B).

Subcellular localization. C6BV and SKNMC/BV were examined by indirect immunofluorescence. Staining of C6BV and SKNMC/BV cells with a rabbit antiserum to BVp40, the viral nucleoprotein, showed that more than 98% of the cells were infected, whereas only 2 to 10% of the cells were labeled with the RbαBVp56 antiserum (not shown). In this case, we observed a fine, reticular staining pattern consistent with typical ER staining. We also observed staining at the nuclear envelope. The same staining pattern was observed among the two BDV-infected cell lines and in CHO cells transfected with the CMV-p56 plasmid (Fig. 5A), indicating that intracellular localization of BVp56 products does not seem to depend on other proteins produced during BDV infection. To further define the subcellular localization of BVp56, we conducted double immunofluorescence experiments using an anti-BiP antibody, an ER-resident protein (47). Confocal microscopy analysis revealed a close colocalization of BVp56 and BiP (Fig. 5A). We also used an anti-mannosidase II antibody, a typical marker of the Golgi complex (22). The staining pattern observed with this antibody was different from the one obtained with RbαBVp56 or anti-BiP antibodies (not shown), indicating that it is unlikely that BVp56 products accumulate in the Golgi complex.

We could not detect staining at the plasma membrane of infected or transfected cells by cell surface immunofluorescence after fixation of the cells with paraformaldehyde or by fluorescence-activated cell sorter analysis (not shown). This could be due to the inability of the RbαBVp56 antiserum to recognize BVp56 products under the native conformation presented at the cell surface. To verify that no BVp56 protein was present at the surface of persistently infected cells, we utilized a cell surface biotinylation assay to differentiate between pro-

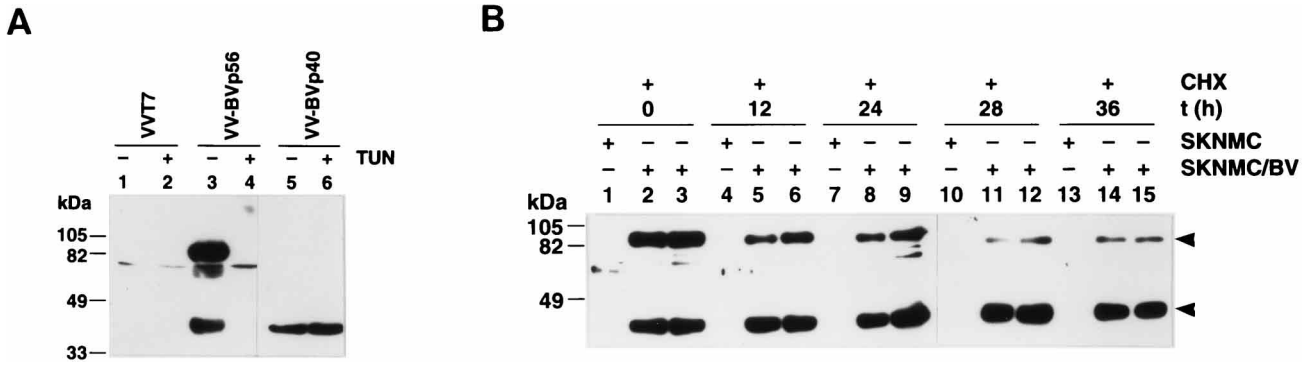

FIG. 3. (A) Effect of TUN. BHK-21 cells were left untreated or treated with TUN before infection with VVT7, VV-BVp56, and VV-BVp40 recombinant vaccinia viruses. Cell extracts were prepared 16 h after infection, and the samples were used for Western blot assays, using the RbαBVp56 antiserum (lanes 1 through 4) or a rabbit anti-BVp40 antibody, diluted 1:25,000 (RbαBVp40, lanes 5 and 6). (B) Treatment with CHX. SKNMC and two separate preparations of SKNMC/BV cells were incubated in the presence or in the absence of CHX. At different times after onset of treatment, whole-cell extracts were prepared and analyzed by Western blotting using the RbαBVp56 antiserum. Arrowheads indicate the positions of GP-84 and GP-43 polypeptides.

teins expressed in the whole cell and on the cell surface. SKNMC/BV cells were reacted with a membrane-impermeable biotinylation reagent, and proteins present at the cell surface were recovered by incubating samples with streptavidin-agarose beads. Samples were then analyzed by Western blotting (Fig. 5B). The validity of this approach was verified by showing that the transferrin receptor molecule could effectively be detected in the cell surface fraction (Fig. 5B, top panel) by using the H-68 antibody (49). In contrast, the BVp40 protein, the counterpart of other NNS RNA virus nucleoproteins, was detected only in whole-cell extract (Fig. 5B, bottom panel). Analysis of the distribution of BVp56 products showed that GP-84 was not detected at the cell surface, consistent with our previous results. However, the GP-43 polypeptide was recovered from the surface fraction (Fig. 5B, central panel).

BVp56 polypeptides are associated with cell-released virus preparations. Next, we wanted to identify which BVp56 products were associated with cell-free infectious BDV virions. Since very little free virus is present in supernatants of persistently BDV-infected cell lines, we isolated cell-released virus particles after submitting cells to a hypertonic treatment (3, 9). The virus was purified on sequential Renografin gradients (discontinuous and continuous). Fractions of the second gradient were assayed for infectivity by using an immunofocus assay (Fig. 6A). The peak of infectivity was found in fractions 3 and 4 of the gradient, corresponding to a density of approximately 1.130 g/ml, consistent with the buoyant density previously reported for BDV particles. Electron microscopy examination after negative staining confirmed the presence of particles ranging from 80 to 130 nm in diameter in these fractions (Fig. 6B). In parallel, an aliquot of each fraction was analyzed by Western blotting, using the RbαBVp56 antiserum (Fig. 6C). GP-84 and GP-43 were concomitantly found in fractions 1 through 5 and decreased simultaneously with the infectivity of the fractions. Thus, both GP-84 and GP-43 seem to be present in infectious particles released from SKNMC/BV cells.

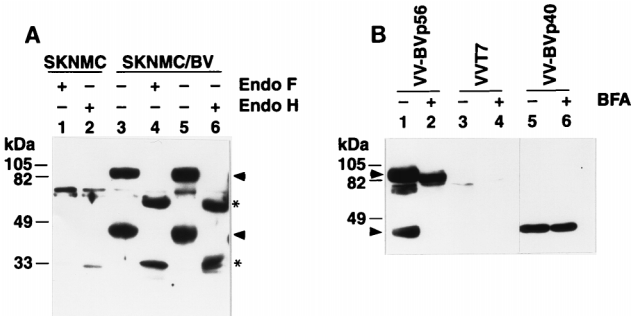

FIG. 4. (A) Digestion with endoglycosidases. Microsomal fractions prepared from SKNMC or SKNMC/BV cells were digested with Endo F and Endo H as described in Materials and Methods. The samples were then analyzed by Western blotting using the RbαBVp56 antiserum. Arrowheads indicate the position of GP-84 and GP-43 polypeptides and stars indicate the position of the products generated by digestion with the endoglycosidases. (B) Treatment with BFA. BHK-21 cells were treated or not with BFA before infection with VV-BVp56, VVT7, and VV-BVp40 recombinant vaccinia viruses. Cell extracts were prepared 16 h after infection, and the samples were used for Western blot assays, using the RbαBVp56 antiserum (lanes 1 through 4) or a rabbit anti-BVp40 antibody (RbαBVp40, lanes 5 and 6).

BVp56 polypeptides are involved in virus cell entry. We also wanted to investigate whether we could neutralize the infectivity of BDV particles by using the RbαBVp56 antiserum. Aliquots (1,000 FFU) of cell-released BDV preparations were incubated for 1 h at 37°C with serial dilutions of various heat-inactivated antisera and assayed for infectivity by immunofocus assay on C6 cells (Fig. 7). The RbαBVp56 antiserum blocked BDV infectivity in a dose-dependent fashion. This effect was not observed with the preimmune serum, suggesting that no other component in the serum is involved. A neutralizing serum directed against vesicular stomatitis virus, another NNS RNA virus, was also unable to block BDV infection. Finally, a rabbit antiserum raised against the BDV p40 protein, which is unlikely to be present at the surface of the virion, did not alter infectivity of viral particles.

DISCUSSION

A knowledge of viral protein transport, assembly, and release is a critical step for a better understanding of the life cycle of a new virus and its pathogenesis in susceptible hosts. Virus propagation within the host is greatly influenced by (i) infection of specific cell types via receptor recognition and (ii) the efficiency of the late steps of the replication cycle, namely the assembly, maturation, and release of infectious virions that will subsequently infect neighboring cells. In the case of enveloped viruses, like BDV, viral surface GPs are key factors governing these processes.

No information is available yet concerning BDV surface GP. The indication that BDV represents a new viral taxon, together with the evidence that BDV can infect humans, possibly being

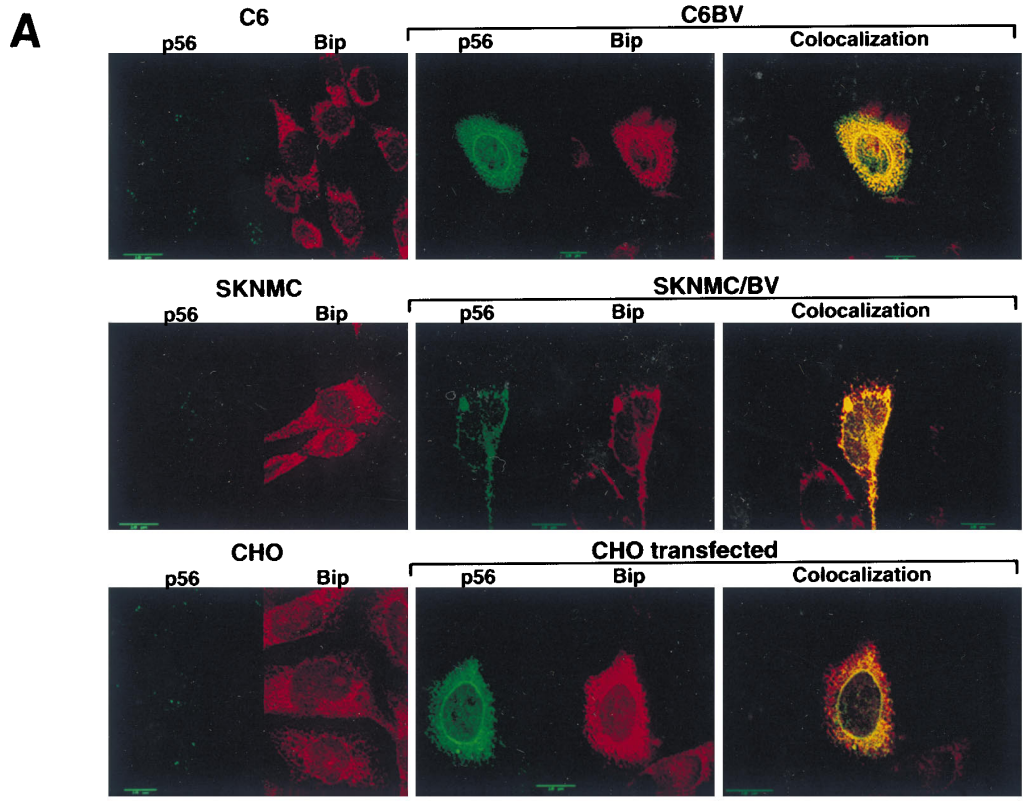
A
C6
p56
Bip
C6BV
p56
Bip
Colocalization
SKNMC
p56
Bip
SKNMC/BV
p56
Bip
Colocalization
CHO
p56
Bip
CHO transfected
p56
Bip
Colocalization

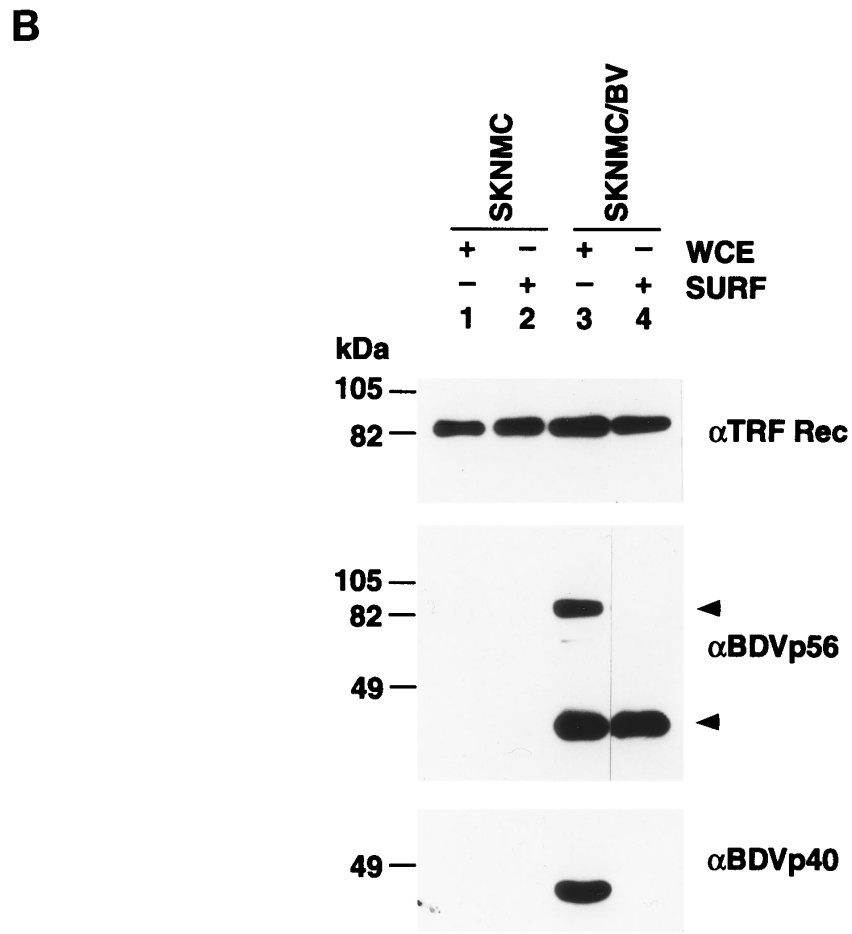
B
SKNMC
SKNMC/BV
+ − + − WCE
− + − + SURF
1 2 3 4
kDa
105
82
αTRF Rec
105
82
49
αBDVp56
49
αBDVp40

associated with certain neuropsychiatric disorders (2, 13, 23, 36, 46), provides further impetus for improving our knowledge about the biology of BDV.

The BDV ORF IV (BVp56) amino acid sequence shares features common to other NNS RNA virus type I transmembrane GPs. These features, together with similarities in genome organization between BDV and other NNS RNA viruses, strongly suggest that BVp56 encodes the virus surface GP. However, BVp56 does not appear to be genetically related to any other NNS RNA virus GP.

Consistent with previous reports (11, 39), we observed that monocistronic mRNA with capability to produce BVp56 was not detected in BDV-infected cells. However, these cells produced detectable levels of BVp56 polypeptides. All the mRNAs potentially coding for BVp56 start upstream of the BVp16 gene, which is encoded in a different reading frame than BVp56. In addition, efficient translation of BVp56 is likely to require RNA splicing (11, 39). Therefore, expression of BVp56 appears to be tightly regulated. This may explain why expression of this protein is restricted in BDV-infected cells, with only 2 to 10% of these cells having levels of BVp56 detectable by immunofluorescence, whereas more than 98% were positive for BVp40 antigen (not shown). Whether this restricted expression of BVp56 contributes to the low production of cell-free virus by BDV-infected cells remains to be elucidated. Also, its low level of expression may explain why BVp56 is not a main target for immune recognition in infected animals.

To study the expression of BVp56 in BDV-infected cells, we generated a rabbit polyclonal antiserum raised against a truncated form of BVp56 (RbαBVp56). By Western blot analysis, we detected two products encoded by the BVp56 gene, designated GP-84 and GP-43. The same pattern was observed in two different cell lines infected with BDV, as well as in BHK-21 cells infected with the VV-BVp56 virus. Experiments using the VV-BVp56-myc virus demonstrated that GP-43 corresponds to the C terminus of BVp56 gene and that, consequently, GP-84 is probably the full-length polypeptide. This N-terminal truncated form of BVp56 could result either from an internal initiation in ORF IV during translation or by a post-translational mechanism, i.e., by cleavage of GP-84. Since there is no internal ATG that could account for generation of GP-43, we favor the hypothesis that this product is generated by cleavage of GP-84. Moreover, treatment with BFA before infection with VV-BVp56 did not prevent GP-84 expression, whereas GP-43 was not detected under these conditions. This finding is difficult to reconcile with the hypothesis that GP-43 results from an internal initiation in the ORF IV and is better explained by the assumption that GP-84 is cleaved to generate GP-43, a process inhibited by BFA treatment. Also, there is a stretch of five arginines located in amino acid positions 245 to 249 of BVp56. This sequence conforms to the minimal consensus sequence (Arg-X-X-Arg) recognized by furin, a cellular calcium-dependent subtilisin-like endoprotease which accumulates in the trans-Golgi network. Furin cleaves many cellular protein precursors as well as many viral GPs (16). These include the gp160 of human immunodeficiency virus (21), the H protein of influenza virus (42), and the F protein of measles virus (48). The hypothesis that cleavage of GP-84 is catalyzed by a cellular protease is consistent with our findings that the same pattern of BVp56 expression was observed in BHK-21 cells infected with the recombinant VV-BVp56, in the absence of any other BDV protein. The contribution of furin to BVp56 processing is currently under study.

With the hypothesis that GP-43 is generated by a furin-mediated cleavage of GP-84, one should expect the generation of a second cleavage product of approximately 41 kDa, corresponding to the amino terminus of GP-84 (amino acids 1 to 249). This product was not detected by Western blot. However, the RbαBVp56 antiserum could recognize a polypeptide corresponding to the first 217 amino acids of BVp56. Therefore, we postulate that the N terminus of GP-84 is rapidly degraded following cleavage.

Subcellular fractionation showed that GP-84 and GP-43 were present in the microsome-enriched fraction and confocal analysis revealed a good colocalization of BVp56 with the BiP protein, an ER-resident chaperone. We also observed staining at the nuclear envelope, although our subcellular fractionation studies showed no detectable expression in the nuclear preparation. We think that this can be explained if BVp56 accumulates in the outer nuclear envelope, which was removed from the nuclear fraction by the procedure used for fractionation.

As the BVp56 sequence contains 13 potential N-linked glycosylation sites, it was expected that the native protein would be glycosylated. The high apparent molecular mass of about 84,000 Da for GP-84, compared to the calculated molecular mass of 56,505 Da for BVp56, is consistent with this hypothesis. Inhibition of glycosylation by treatment with TUN completely prevented the detection of GP-84 and, as a consequence, of GP-43. This finding suggests that glycosylation is required for proper folding of the nascent glycopeptide chains, a process already described for other viral surface GPs, like the lymphocytic choriomeningitis virus GP-1 protein (53).

Most of the oligosaccharides attached to BVp56 products appeared to be N-linked glycans, since digestion with Endo F reduced the apparent molecular mass of GP-84 to about 56 kDa, which is close to the predicted molecular mass for BVp56. Although evidence for a strict consensus sequence has not been defined for O glycosylation, several features such as small clusters of hydroxyamino acids (serine and threonine) close to a proline residue indicating turn or loop regions seem to be important (28). Such motifs were not identified in BVp56 sequence. Only three stretches of serine/threonine residues were found in BVp56, two located in the middle part of the sequence (positions 203 and 226) and one towards the C terminus (position 440). These stretches overlap with potential N-glycosylation sites in two out of these three cases. Therefore, it seems rather unlikely that O-glycans contribute significantly to glycosylation of these polypeptides. Also, it is noteworthy that digestion of GP-43 with Endo F yielded a product with a molecular masses of about 27 to 29 kDa. The size of this

FIG. 5. Subcellular localization of BVp56-encoded products. (A) Immunofluorescence assay and confocal analysis. C6, C6BV, SKNMC, SKNMC/BV, and CHO cells, as well as CHO cells transfected with the CMV-BVp56 plasmid, were analyzed by immunofluorescence assay for BVp56 or BiP immunoreactivity (antibody used indicated on top of each panel). BVp56 expression was detected with a FITC-labeled secondary antibody (green), while BiP expression was detected with a Texas red-labeled antibody (red). Colocalization of staining, reflected by a yellow signal, was performed by confocal analysis. No expression was seen when the preimmune rabbit serum was used (not shown). (B) Cell surface biotinylation assay. Cell surface proteins from SKNMC and SKNMC/BV cells were biotinylated and immunoprecipitated with streptavidin-agarose beads as described in Materials and Methods. Aliquots of these preparations (SURF, lanes 2 and 4), as well as equivalent amounts of whole-cell extracts (WCE, lanes 1 and 3) were analyzed by Western blotting, using an anti-transferrin receptor antibody, as well as the RbαBVp56 and RbαBVp40 antisera (antibodies indicated on the right). Arrowheads indicate the positions of GP-84 and GP-43 polypeptides.

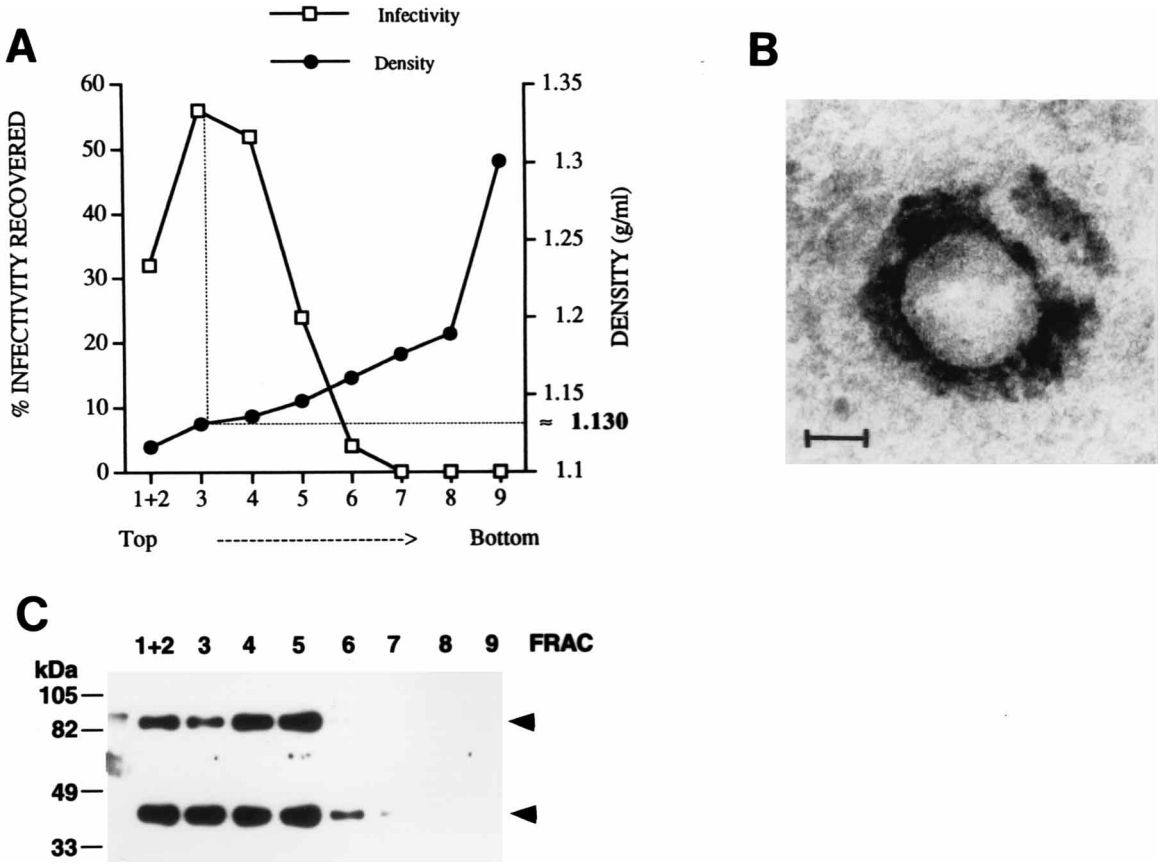

FIG. 6. Cell-released virus analysis. (A) Cell-released virus was prepared from SKNMC/BV cells by sequential Renografin gradients as described in Materials and Methods. The density of each fraction of the second continuous Renografin gradient was determined (black circles). In parallel, aliquots of each fraction were assayed for infectivity by immunofocus assay (open squares). (B) Electron microscopy analysis of the virus-containing fractions. An aliquot of fraction 3 was spotted onto a carbon-coated grid and processed for electron microscopy after negative staining. The figure shows a typical particle observed in these samples. Magnification, ×300,000. (C) Western blot assay. Equivalent amounts of each gradient fraction were analyzed by using the RbαBVp56 antiserum. Arrowheads indicate the positions of GP-84 and GP-43 polypeptides.

product is consistent with the calculated molecular mass of 27,644 Da of the product that would be generated by cleavage at the arginine-rich region located in positions 245 to 249 in the BVp56 sequence.

Unexpectedly, both products were also Endo H sensitive. Susceptibility to Endo H is commonly used to follow the transport of newly synthesized glycoproteins from the ER to the Golgi apparatus, since in the latter compartment most oligosaccharides become resistant to Endo H (29). However, some mature glycoproteins still possess high-mannose chains and retain Endo H susceptibility. Also some viral glycoproteins, such as the G1 and G2 glycoproteins of Hantaan virus, retain Endo H sensitivity even if they accumulate in the Golgi apparatus (33). Therefore, our results do not allow us to discriminate between the possibility that the BVp56 products do not transit through the Golgi, and the possibility that they actually reach the Golgi but do not undergo maturation of their oligosaccharide side chains. On the other hand, retention in the ER by BFA treatment blocked the late stages of glycosylation of GP-84 and completely prevented the production of GP-43. This indicates that after synthesis in the ER, GP-84 has to reach a post-ER compartment for the production of GP-43. Furthermore, the possibility that the cellular protease furin may be responsible for the cleavage of GP-84 to generate GP-43 would favor a transit of BVp56 products in the trans-Golgi network (TGN). Therefore, we postulate that after its synthesis in the ER, a fraction of GP-84 remains in the ER and at the nuclear envelope, whereas another fraction follows the normal biosynthetic pathway, reaches the Golgi without maturation of its oligosaccharide side chains, and is cleaved in the TGN to generate GP-43, which subsequently reaches the cell surface.

The presence of GP-43 at the cell surface was demonstrated by cell surface biotinylation assays. This was achieved by precipitation of cell surface biotinylated proteins with streptavidin-agarose, followed by Western blot analysis of eluted protein under denaturing electrophoresis conditions. In contrast, the immunofluorescence and fluorescence-activated cell sorter procedures used to detect BVp56 products at the cell surface were based on the ability of the RbαBVp56 antiserum to detect these proteins under native conformation. This would explain the apparent discrepancy between immunofluorescence and cell surface biotinylation results.

All other known animal NNS RNA viruses mature at the cell surface of the infected cell. Moreover, most of them express a single GP, although paramyxoviruses have two surface GPs (HN and F). In this case however, these two polypeptides are expressed from different genes. The presence of two GPs, also encoded from distinct ORFs, has also been reported for bovine ephemeral fever rhabdovirus (45). In filoviruses, a smaller product encoded from the GP gene is secreted by infected cells and has an unclear function, possibly immunosuppressive

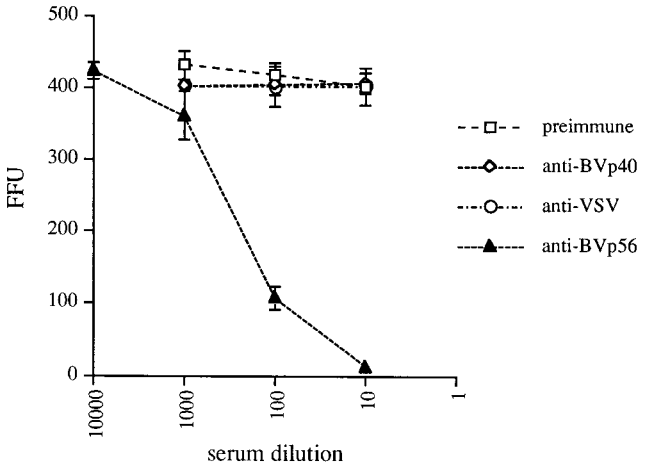

FIG. 7. Seroneutralization assays. Aliquots (1,000 FFU) of purified cell-released BDV were incubated for 1 h at 37°C with serial dilutions of various heat-inactivated antisera and assayed for infectivity by immunofocus on C6 cells. The number of FFU for each dilution represents the mean ± standard deviation of three separate experiments.

properties (30). However, this product results from a regulation mechanism, involving translation in two separate ORFs linked by transcriptional editing (35). In the case of BDV, our data suggest that generation of GP-43 results from cleavage by a cellular protease, a situation observed only for F proteins of NNS RNA viruses.

We also wanted to gain insight into the role that BVp56 polypeptides play in the life cycle of the virus. We found that both GP-43 and GP-84 polypeptides are associated with cell-released infectious virions. We cannot completely exclude the possibility of a contamination of our virus preparations by membrane-bound proteins that would not actually be present in the virion. However, the procedures used to prepare cell-released BDV infectious particles (see details in Materials and Methods) should have prevented or at least minimized such a contamination. The precise mechanisms for assembly of BDV, as well as the contribution of BVp56-encoded polypeptides in determining the localization of such processes, remain to be documented. Nevertheless, we speculate that an early step in BDV assembly may be the incorporation of GP-84 into the viral envelope, acquired during budding of BDV ribonucleoparticles at the nuclear envelope and ER. This would be consistent with the intracellular localization of GP-84. Subsequent routes followed by these particles as they travel out of the cell are unknown. Incorporation of GP-43 into infectious virions may occur at the plasma membrane, during a final step of BDV egress from the infected cell. However, it is also possible that the presence of GP-43 in infectious virions does not represent a normal step in the life cycle of BDV but is rather a consequence of the hypertonic treatment used to increase the yield of cell-released virus. The scarcity of virus particles in the BDV-infected cells used for electron microscopy analysis of thin sections (8) may explain why budding of BDV from either the nuclear envelope, ER, or plasma membrane has not been observed yet. The use of cell culture systems producing higher yields of infectious BDV particles should allow elucidation of the details of BDV assembly process.

The finding that the RbαBVp56 antiserum is neutralizing indicates that BVp56 proteins are involved in the initial steps of infection by BDV. Studies in animal models suggested that one of the primary routes of infection by BDV might be through the olfactory neuroepithelium (18, 26, 32). This initial infection is likely to require interaction between BVp56 and a cellular receptor, yet unidentified. However, subsequent propagation within the CNS may not require expression of BDV surface GP. BDV ribonucleoparticles (RNP) are infectious (9) and evidence suggests that they may contribute to the viral spread of the virus within the CNS (19), without requiring generation of mature particles. Restricted expression of BVp56 may explain the low production of cell-free virus in vivo and in vitro. This, in turn, may account for the low rate of contagion associated with BDV, since there is no outbreak associated with BDV infection and natural cases of Borna disease are always sparse. It may also constitute a mechanism by which BDV evades neutralization by the host immune response. A better understanding of the regulation of expression of BVp56 and of its potential role in controlling virus production and spread will contribute to improving our knowledge about this novel neurotropic infectious agent with possible implications for human health.

ACKNOWLEDGMENTS

This work was supported by grant NS 32355-02 (J.C.T.), by the Institut Pasteur, and by a grant from the North Atlantic Treaty Organization (D.G.-D.).

We thank C. Sauder and A. Müller for assistance in the generation of the RbαBVp56 antiserum, S. Boullier for help in fluorescence-activated cell sorter analysis. G. Klier for confocal microscope analysis, and I. Dunia and E. L. Benedetti for electron microscopy. We also thank J. L. Whitton for his help in the generation of the recombinant vaccinia viruses, as well as C. Oldstone and H. Perkins for assistance. P. Borrow, N. Mackman, C. Sauder, and I. Novella are gratefully acknowledged for critically reading the manuscript.

REFERENCES

1. **Ausubel, F. M., R. Brent, R. E. Kingston, D. D. Moore, J. G. Seidman, J. A. Smith, and K. Struhl.** 1992. Current protocols in molecular biology. Greene Publishing Associates and Wiley-Interscience, New York.
2. **Bode, L.** 1995. Human infections with Borna disease virus and potential pathogenic implications, p. 103–130. *In* H. Koprowski and I. Lipkin (ed.), Borna disease. Springer-Verlag, Berlin, Germany.
3. **Briese, T., J. C. de la Torre, A. Lewis, H. Ludwig, and W. I. Lipkin.** 1992. Borna disease virus, a negative-strand RNA virus, transcribes in the nucleus of infected cells. Proc. Natl. Acad. Sci. USA **89:**11486–11489.
4. **Briese, T., A. Schneemann, A. J. Lewis, Y. S. Park, S. Kim, H. Ludwig, and W. I. Lipkin.** 1994. Genomic organization of Borna disease virus. Proc. Natl. Acad. Sci. USA **91:**4362–4366.
5. **Carbone, K. M., S. A. Rubin, A. M. Sierra-Honigmann, and H. M. Lederman.** 1993. Characterization of a glial cell line persistently infected with borna disease virus (BDV): influence of neurotrophic factors on BDV protein and RNA expression. J. Virol. **67:**1453–1460.
6. **Chakrabarti, S., K. Brechling, and B. Moss.** 1985. Vaccinia virus expression vector: coexpression of beta-galactosidase provides visual screening of recombinant virus plaques. Mol. Cell. Biol. **5:**3403–3409.
7. **Chatterjee, S., and S. Sarkar.** 1992. Studies on endoplasmic reticulum—Golgi complex cycling pathway in herpes simplex virus-infected and brefeldin A-treated human fibroblast cells. Virology **191:**327–337.
8. **Compans, R. W., L. R. Melsen, and J. C. de la Torre.** 1994. Virus-like particles in MDCK cells persistently infected with Borna disease virus. Virus Res. **33:**261–268.
9. **Cubitt, B., and J. C. de la Torre.** 1994. Borna disease virus (BDV), a nonsegmented RNA virus, replicates in the nuclei of infected cells where infectious BDV ribonucleoproteins are present. J. Virol. **68:**1371–1381.
10. **Cubitt, B., C. Oldstone, and J. C. de la Torre.** 1994. Sequence and genome organization of Borna disease virus. J. Virol. **68:**1382–1396.
11. **Cubitt, B., C. Oldstone, J. Valcarcel, and J. C. de la Torre.** 1994. RNA splicing contributes to the generation of mature mRNAs of Borna disease virus, a non-segmented negative strand RNA virus. Virus Res. **34:**69–79.
12. **de la Torre, J. C.** 1994. Molecular biology of borna disease virus: prototype of a new group of animal viruses. J. Virol. **68:**7669–7675.
13. **de la Torre, J. C., D. Gonzalez-Dunia, B. Cubitt, M. Mallory, N. Mueller-Lantzsch, F. A. Grässer, L. A. Hansen, and E. Masliah.** 1996. Detection of Borna Disease virus antigen and RNA in human autopsy brain samples from neuropsychiatric patients. Virology **223:**272–282.
14. **Fields, B. N., D. M. Knipe, P. M. Howley, R. M. Chanock, J. L. Melnick, T. P.**

Monath, B. Roizman, and S. E. Straus. 1996. Fields virology. Lippincott-Raven, Philadelphia, Pa.
15. **Fuerst, T. R., E. G. Niles, F. W. Studier, and B. Moss.** 1986. Eukaryotic transient expression system based on recombinant vaccinia virus that synthesizes bacteriophage T7 RNA polymerase. Proc. Natl. Acad. Sci. USA **83:**8122–8126.
16. **Garten, W., S. Hallenberger, D. Ortmann, W. Schafer, M. Vey, H. Angliker, E. Shaw, and H. D. Klenk.** 1994. Processing of viral glycoproteins by the subtilisin-like endoprotease furin and its inhibition by specific peptidylchloroalkylketones. Biochimie **76:**217–225.
17. **Gonzalez-Dunia, D., M. Eddleston, N. Mackman, K. Carbone, and J. C. de la Torre.** 1996. Expression of tissue factor is increased in astrocytes within the central nervous system during persistent infection with Borna disease virus. J. Virol. **70:**5812–5820.
18. **Gosztonji, G., and H. Ludwig.** 1995. Borna disease—neuropathology and pathogenesis, p. 39–73. *In* H. Koprowski and I. Lipkin (ed.), Borna disease. Springer-Verlag, Berlin, Germany.
19. **Gosztonyi, G., B. Dietzschold, M. Kao, C. E. Rupprecht, H. Ludwig, and H. Koprowski.** 1993. Rabies and borna disease. A comparative pathogenetic study of two neurovirulent agents. Lab. Invest. **68:**285–295.
20. **Gregory, D. W., and B. J. Pirie.** 1973. Wetting agents for biological electron microscopy. I. General considerations and negative staining. J. Microsc. **99:**251–255.
21. **Hallenberger, S., V. Bosch, H. Angliker, E. Shaw, H. D. Klenk, and W. Garten.** 1992. Inhibition of furin-mediated cleavage activation of HIV-1 glycoprotein gp160. Nature **360:**358–361.
22. **Hobman, T. C., L. Woodward, and M. G. Farquhar.** 1993. The rubella virus E2 and E1 spike glycoproteins are targeted to the Golgi complex. J. Cell. Biol. **121:**269–281.
23. **Kishi, M., Y. Arimura, K. Ikuta, Y. Shoya, P. K. Lai, and M. Kakinuma.** 1996. Sequence variability of Borna disease virus open reading frame II found in human peripheral blood mononuclear cells. J. Virol. **70:**635–640.
24. **Koerner, T. J., J. E. Hill, A. M. Myers, and A. Tzagoloff.** 1991. High-expression vectors with multiple cloning sites for construction of trpE fusion genes: pATH vectors. Methods Enzymol. **194:**477–90.
25. **Lamb, R. A., and D. Kolakofsky.** 1996. Paramyxoviridae: the viruses and their replication, p. 1177–1204. *In* B. N. Fields, D. M. Knipe, P. M. Howley, R. M. Chanock, J. L. Melnick, T. P. Monath, B. Roizman, and S. E. Straus (ed.), Fields virology. Lippincott-Raven, Philadelphia, Pa.
26. **Ludwig, H., L. Bode, and G. Gosztonji.** 1988. Borna disease: a persistent virus infection of the central nervous system. Prog. Med. Virol. **35:**107–151.
27. **Nicolau, S., and I. A. Galloway.** 1928. Borna disease and enzootic encephalomyelitis of sheep and cattle. Special Report Series, Med. Res. Council **121:**7–90.
28. **Niemann, H., R. Geyer, H. D. Klenk, D. Linder, S. Stirm, and M. Wirth.** 1984. The carbohydrates of mouse hepatitis virus (MHV) A-59: structures of O-glycosidically linked oligosaccharides of glycoprotein E1. EMBO J. **3:**665–670.
29. **Paterson, R. G., and R. A. Lamb.** 1993. The molecular biology of influenza viruses and paramyxoviruses, p. 35–73. *In* A. J. Davison and R. M. Elliott (ed.), Molecular virology—a practical approach. IRL Press, Oxford, United Kingdom.
30. **Peters, C. J., A. Sanchez, P. E. Rollin, T. G. Ksiazek, and F. A. Murphy.** 1996. Filoviridae: Marburg and Ebola viruses, p. 1161–1176. *In* B. N. Fields, D. M. Knipe, P. M. Howley, R. M. Chanock, J. L. Melnick, T. P. Monath, B. Roizman, and S. E. Straus (ed.), Fields virology. Lippincott-Raven, Philadelphia, Pa.
31. **Pettersson, R. F.** 1991. Protein localization and virus assembly at intracellular membranes, p. 67–106. *In* R. W. Compans (ed.), Protein traffic in eucaryotic cells. Springer-Verlag KG, Berlin, Germany.
32. **Rott, R., and H. Becht.** 1995. Natural and experimental Borna disease in animals, p. 17–30. *In* H. Koprowski and I. Lipkin (Ed.), Borna disease. Springer-Verlag, Berlin, Germany.
33. **Ruusala, A., R. Persson, C. S. Schmaljohn, and R. F. Pettersson.** 1992. Coexpression of the membrane glycoproteins G1 and G2 of Hantaan virus is required for targeting to the Golgi complex. Virology **186:**53–64.
34. **Sambrook, J., E. F. Fritsch, and T. Maniatis.** 1989. Molecular cloning: a laboratory manual, 2nd ed. Cold Spring Harbor Laboratory Press, Cold Spring Harbor, N.Y.
35. **Sanchez, A., S. G. Trappier, B. W. Mahy, C. J. Peters, and S. T. Nichol.** 1996. The virion glycoproteins of Ebola viruses are encoded in two reading frames and are expressed through transcriptional editing. Proc. Natl. Acad. Sci. USA **93:**3602–3607.
36. **Sauder, C., A. Müller, B. Cubitt, J. Mayer, J. Steinmetz, W. Trabert, B. Ziegler, K. Wanke, N. Mueller-Lantzsch, J. C. de la Torre, and F. A. Grässer.** 1996. Detection of Borna disease virus (BDV) antibodies and BDV RNA in psychiatric patients: evidence for high sequence conservation of human blood-derived BDV RNA. J. Virol. **70:**7713–7724.
37. **Schlesinger, M. J., and S. Schlesinger.** 1987. Domains of virus glycoproteins. Adv. Virus Res. **33:**1–44.
38. **Schneemann, A., P. A. Schneider, R. A. Lamb, and W. I. Lipkin.** 1995. The remarkable coding strategy of borna disease virus: a new member of the nonsegmented negative strand RNA viruses. Virology **210:**1–8.
39. **Schneider, P. A., A. Schneemann, and W. I. Lipkin.** 1994. RNA splicing in Borna disease virus, a nonsegmented, negative-strand RNA virus. J. Virol. **68:**5007–5012.
40. **Spies, C. P., and R. W. Compans.** 1993. Alternate pathways of secretion of simian immunodeficiency virus envelope glycoproteins. J. Virol. **67:**6535–6541.
41. **Squinto, S. P., T. H. Aldrich, R. M. Lindsay, D. M. Morrissey, N. Panayotatos, S. M. Bianco, M. E. Furth, and G. D. Yancopoulos.** 1990. Identification of functional receptors for ciliary neurotrophic factor on neuronal cell lines and primary neurons. Neuron **5:**757–766.
42. **Stieneke-Grober, A., M. Vey, H. Angliker, E. Shaw, G. Thomas, C. Roberts, H. D. Klenk, and W. Garten.** 1992. Influenza virus hemagglutinin with multibasic cleavage site is activated by furin, a subtilisin-like endoprotease. EMBO J. **11:**2407–2414.
43. **Takatsuki, A., and G. Tamura.** 1985. Brefeldin A, a specific inhibitor of intracellular translocation of vesicular stomatitis virus G protein: intracellular accumulation of high-mannose type G protein and inhibition of its cell surface expression. Agric. Biol. Chem. **48:**899–902.
44. **Wagner, R. R., and J. K. Rose.** 1996. Rhabdoviridae: the viruses and their replication, p. 1121–1135. *In* B. N. Fields, D. M. Knipe, P. M. Howley, R. M. Chanock, J. L. Melnick, T. P. Monath, B. Roizman, and S. E. Straus (ed.), Fields virology. Lippincott-Raven, Philadelphia, Pa.
45. **Walker, P. J., K. A. Byrne, G. A. Riding, J. A. Cowley, Y. Wang, and S. McWilliam.** 1992. The genome of bovine ephemeral fever rhabdovirus contains two related glycoprotein genes. Virology **191:**49–61.
46. **Waltrip, R. W., II, R. W. Buchanan, A. Summerfelt, A. Breier, W. T. Carpenter, N. Bryant, S. A. Rubin, and K. M. Carbone.** 1995. Borna disease virus and schizophrenia. Psychiatry Res. **56:**33–44.
47. **Warren, G.** 1987. Protein transport. Signals and salvage sequences. Nature **327:**17–18.
48. **Watanabe, M., A. Hirano, S. Stenglein, J. Nelson, G. Thomas, and T. C. Wong.** 1995. Engineered serine protease inhibitor prevents furin-catalyzed activation of the fusion glycoprotein and production of infectious measles virus. J. Virol. **69:**3206–3210.
49. **White, S., K. Miller, C. Hopkins, and I. S. Trowbridge.** 1992. Monoclonal antibodies against defined epitopes of the human transferrin receptor cytoplasmic tail. Biochim. Biophys. Acta **1136:**28–34.
49a. **Whitton, J. L.** Personal communication.
50. **Whitton, J. L., P. J. Southern, and M. B. Oldstone.** 1988. Analyses of the cytotoxic T lymphocyte responses to glycoprotein and nucleoprotein components of lymphocytic choriomeningitis virus. Virology **162:**321–327.
51. **Whitton, J. L., and A. Tishon.** 1990. Detection, generation and use of cytotoxic T-lymphocytes (CTL) clones-4C. Use in vitro to map CTL epitopes, p. 104–115. *In* M. B. A. Oldstone (ed.), Animal virus pathogenesis. IRL Press, Oxford, United Kingdom.
52. **Wickner, W. T., and H. F. Lodish.** 1985. Multiple mechanisms of protein insertion into and across membranes. Science **230:**400–407.
53. **Wright, K. E., M. S. Salvato, and M. J. Buchmeier.** 1989. Neutralizing epitopes of lymphocytic choriomeningitis virus are conformational and require both glycosylation and disulfide bonds for expression. Virology **171:** 417–426.
54. **Zimmermann, W., H. Breter, M. Rudolph, and H. Ludwig.** 1994. Borna disease virus: immunoelectron microscopic characterization of cell-free virus and further information about the genome. J. Virol. **68:**6755–6758.